Electronic Supplementary Material (ESI) for Lab on a Chip

Supplementary Information for
"Sucrose-based fabrication of 3D-networked, cylindrical microfluidic channel for rapid-prototyping of lab-on-a-chip and vaso-mimetic device"

Jiwon Lee, Jungwook Paek and Jaeyoun Kim*

1. Sucrose template shaping

The sucrose fibers were shaped to form 3D sacrificial templates. Sucrose fibers with diameter < 50 μm are flexible enough to be shaped into diverse 3D forms at room temperature directly. To assist the shaping process, we often used pre-made PDMS blocks. Figure S1 shows a pilot fabrication of a solenoidal MF channel through coiling a ~25 μm-thick sucrose fiber around a 1.7 mm-diameter PDMS cylinder and then embedding the assembly in liquid PDMS. As the two PDMS coagulate over the curing process, the solenoidal channel ends up in a monolithic PDMS block. As the sucrose fibers get stiffer with increasing diameter, shaping thicker fibers requires heating and/or moisturization.

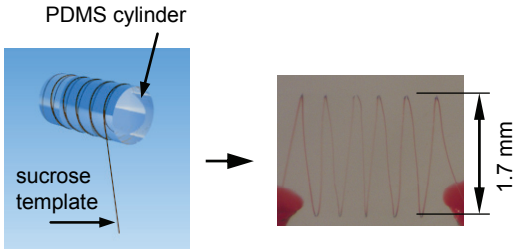

Fig. S1 An example in which a solenoidal MF channel is fabricated using a PDMS cylinder

2. Sucrose template assembly and molding

The formation of complex 3D trajectories with sucrose fibers, especially the ones with diameter < 100 μm that tend to sag, can be facilitated greatly if pre-made PDMS blocks were used as props or supports. As the PDMS core used for solenoidal MF channels, the PDMS blocks coagulate with the second batch and become a part of the final LoCs. In preparing the PDMS blocks, care was taken to keep their surfaces pristine to guarantee clean coagulation. A PDMS pillar array, shown in Fig. S2a, also helped outlaying the sucrose fibers before bonding. The pillars are 450 and 200 μm in diameter and height, respectively, and made with standard PDMS molding of a SU-8 master. The gap between the pillars, 300 μm in width, provides space for placing and aligning sucrose templates with diameter between 100 and 300 μm. As show in Fig. S2a, other sucrose fiber templates can also be placed at an angle to the original one. The restraint and guidance afforded by the PDMS pillars greatly facilitated the aligning, bonding, and assembly processes. Once the assembly was completed, the PDMS pillar array and the sucrose fibers were placed in a container to be filled with uncured PDMS so that the PDMS-PDMS coagulation process can combine the two PDMS structures.

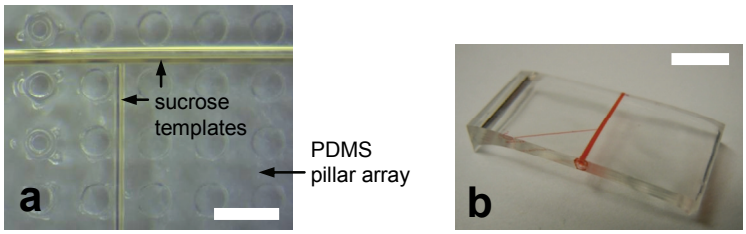

Fig. S2 (a) A PDMS pillar array assisting the assembly of sucrose fiber templates (scale bar: 1 mm) (b) A 3D MF channel network fabricated in PU (NOA73). (scale bar: 5 mm).

The completed template assembly (Fig. 1e) can be steam-annealed again to reduce surface roughness or residues. Then the sucrose template assembly, possibly including PDMS blocks, were put into a container to be filled with the 10:1 mixture of PDMS base and hardener (Fig. 1f). Upon complete curing of PDMS, the sucrose fiber assembly was dissolved in water at 70°C and the channel was filled with red dye (Fig. 1g). This low temperature for template removal allows the use of poly urethane (PU), a UV curable polymer (NOA73, Norland). We first made a base layer by filling the container with PU at 1 mm depth and exposing it to UV light (S1000, Omnicure) at 20 mW/cm^2 for 80 seconds. Then we placed the sucrose assembly on the PU layer, poured more PU, and exposed it again at 20 mW/cm^2 for 100 seconds. Figure S2b shows one completed pilot PU-based MF device.

3. Physical characteristics of sucrose templates

Figures S3a to d show the microscope images of the sucrose fibers pulled at 25.6, 8.5, 3.4, and 2.0 cm/s, respectively, in both side and cross-sectional views. The first and the last one are present in Fig. 2 but repeated here for easier comparison.

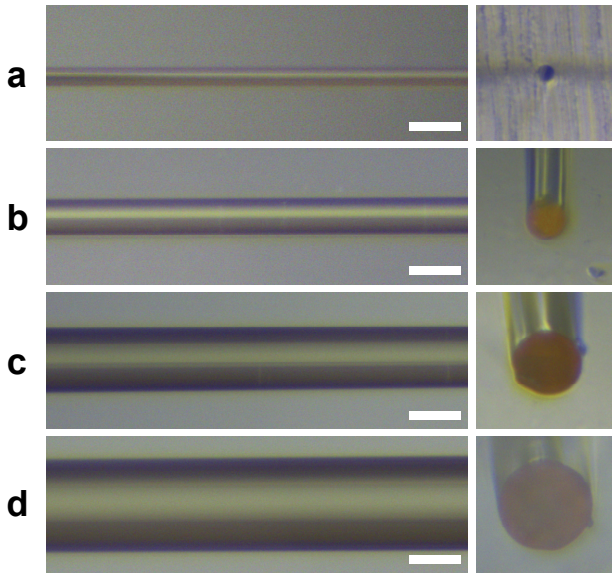

Fig. S3 Side and cross-sectional images of sucrose fibers pulled at 25.6, 8.5, 3.4, and 2.0 cm/s (scale bar: 200 μm).

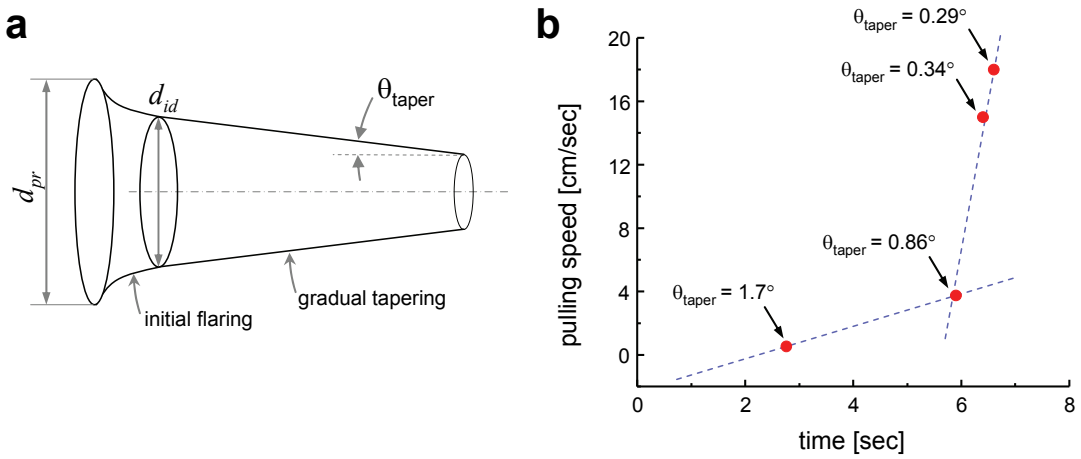

Fig. S4 (a) A typical tapered sucrose fiber geometry with the definitions of the taper angle θ_{taper}, the pulling rod diameter (d_{pr}), and the initial desired diameter (d_{id}). (b) A typical pattern in the speed of pulling as a function of the time and the corresponding values of θ_{taper}.

4. Tapering of the sucrose fiber templates

The diameters of the sucrose fibers drawn at constant pulling speeds, shown in Fig. 2c, were uniform along the length of the fibers. In 3D microfluidic networks, the tapered channel is an essential element of the 3D microfluidic network. Fabrication of 3D, cylindrically tapered channels in PDMS, however, has been technically challenging so far with very few published reports. This sucrose-based technique greatly facilitated their fabrication thanks to the fact that the sucrose fiber's diameter can be varied continuously. One example is the template for the backbone channel shown in Fig. 3e which exhibits a clearly visible tapering with the θ_{taper} = 0.44° taper angle as defined in Fig. S4. Other values of θ_{taper} were also achieved by varying the pulling conditions.

Among many parameters of the pulling process, the level of tapering was most strongly affected by two factors: the pulling rod diameter and the acceleration in the pulling speed. Figure S4b shows a typical result. At first, the fiber was drawn slowly until the desired value of diameter was reached. The first two data points correspond to this initial regime. In this regime, the tapering is highly curved as shown in Fig. S4a. The degree of this *flaring* is mainly governed by the difference between the pulling rod diameter d_{pr} and the initial desired fiber diameter d_{id}. Then we applied a constant acceleration to achieve a gradual taper. The last three data points represent this linear ramping regime. The corresponding values of θ_{taper} indicate that the level of tapering became lower as the fiber length increased. To clarify the relation between this linear ramping and the degree of tapering, we pulled several 2 cm-long sucrose fibers with different degrees of ramping. The results, summarized in Table 1S, indicate that a higher acceleration in ramping speed does *not* always lead to a higher degree of tapering. In the linear regime, the tapering angle saturates at around 0.5°, which agrees with the result shown in Fig. 3e.

Ramp [cm/s^2]	θ_{taper}
1.20	0.39
1.23	0.34
1.79	0.55
20.0	0.49

Table 1S Ramp vs. taper angle